



Using mathematical modeling to estimate time-independent cancer chemotherapy efficacy parameters

Christine Pho¹ · Madison Frieler² · Giri R. Akkaraju² · Anton V. Naumov¹ · Hana M. Dobrovolny¹

Received: 5 October 2021 / Accepted: 19 November 2021

© The Author(s), under exclusive licence to Springer-Verlag GmbH Germany, part of Springer Nature 2021

Abstract

One of the primary cancer treatment modalities is chemotherapy. Unfortunately, traditional anti-cancer drugs are often not selective and cause damage to healthy cells, leading to serious side effects for patients. For this reason more targeted therapeutics and drug delivery methods are being developed. The effectiveness of new treatments is initially determined via in vitro cell viability assays, which determine the IC_{50} of the drug. However, these assays are known to result in estimates of IC_{50} that depend on the measurement time, possibly resulting in over- or under-estimation of the IC_{50} . Here, we test the possibility of using cell growth curves and fitting of mathematical models to determine the IC_{50} as well as the maximum efficacy of a drug (ϵ_{max}). We measured cell growth of MCF-7 and HeLa cells in the presence of different concentrations of doxorubicin and fit the data with a logistic growth model that incorporates the effect of the drug. This method leads to measurement time-independent estimates of IC_{50} and ϵ_{max} , but we find that ϵ_{max} is not identifiable. Further refinement of this methodology is needed to produce uniquely identifiable parameter estimates.

Keywords Mathematical model · Parameter estimation · Data fitting · Chemotherapy · Drug efficacy

Introduction

Cancer is the second leading cause of mortality worldwide (Bray et al. 2018). One of the primary treatment strategies currently in use is chemotherapy that is often effective against tumors, however, can also detrimentally affect the healthy tissues (Miller et al. 2016). New, cancer-targeted approaches are continuously being developed (Tang and Zhao 2020; Peng et al. 2020), as are new nanotechnology-based delivery mechanisms for existing drugs (Rejinold et al. 2020; Khan et al. 2020). These potential new treatments

need to be well-tested and characterized in vitro (Gurney 2002) before being considered for use in patients.

The most common method for determining the effectiveness of a drug is by administering different concentrations of the potential chemotherapeutic to cancer cells in order to generate a dose response curve. The dose response curve yields the IC_{50} , which is the drug concentration needed to achieve half the maximum effect of the drug. Although not often measured, the dose–response curve also yields ϵ_{max} , which is the maximum effect of the drug. Unfortunately, dose–response curves generated in this way can be problematic. There are known sensitivities to experimental details (Larsson et al. 2020) that can lead to variation in measurements. Measurement error is often not accounted for when using the dose response curve to estimate IC_{50} , which can lead to incorrect IC_{50} estimates (Wang et al. 2021). Additionally, dose response curves also provide IC_{50} and ϵ_{max} estimates that depend on the measurement time (Murphy et al. 2020; Harris et al. 2016; Hafner et al. 2016), and are unable to yield the correct value of both measurements with a single measurement time (Murphy et al. 2020). An incorrect estimate of IC_{50} and ϵ_{max} leads to the potential for over- or under-dosing as new drugs move from in vitro to animal and human studies (Kurilov et al. 2020; Bae et al. 2020). This

✉ Hana M. Dobrovolny
h.dobrovolny@tcu.edu

Giri R. Akkaraju
g.akkarakaju@tcu.edu

Anton V. Naumov
a.naumov@tcu.edu

¹ Department of Physics and Astronomy, Texas Christian University, 2800 S. University Drive, Fort Worth 76129, TX, USA

² Department of Biology, Texas Christian University, 2800 S. University Drive, Fort Worth 76129, TX, USA

can result in either underestimation of the toxic effect of the drug and increased animal mortality in further in vivo experiments or prevent effective therapeutics and nanoformulations from further developing into treatment mechanisms.

A variety of alternative measurements have been proposed, such as using additional features of the dose–response curve like area under the curve (AUC) or the slope of the curve, for a more complete characterization of the effect of a drug (Fallahi-Sichani et al. 2013; Brooks et al. 2019). Another suggestion is to use other points on the dose response curve such as the minimal response or the dose with the maximum affinity in the response reaction (Calhella et al. 2017; Brooks et al. 2019). There is also a new assay that separately measures a drug's effect on cell death from the drug's effect on cell growth, calculating separate IC_{50} for each (Bae et al. 2020) together with suggestions of using both positive and negative controls to normalize drug response measurements (Gupta et al. 2020). Unfortunately, these suggestions still use dose–response curves generated by measuring the number of cells on a particular day and these additional measures might suffer from the same time-dependence issue as IC_{50} and ϵ_{max} .

A more promising suggestion is to use measurements of growth rate (GR) in order to generate dose–response curves (Hafner et al. 2016; Harris et al. 2016; Niepel et al. 2019). Growth rate is largely independent of measurement time after a short transient phase and before the plateau (Harris et al. 2016). Thus, dose–response curves can be generated that result in consistent GR_{50} and GR_{max} estimates (Hafner et al. 2016). While this is a promising idea, experimental data must be taken after the initial transient phase, and, thus there have been problems with implementing this technique in a manner that is reproducible in different research centers (Niepel et al. 2019).

The use of mathematical modeling and computer simulation has become increasingly important to the development of pharmaceuticals (Zhang et al. 2006). Pharmacokinetic models have long been used to predict absorption and elimination of pharmaceutical compounds in the body (Chen et al. 2012). These models are increasingly being linked to physiological models to assess both the effectiveness of a drug, as well as possible side effects (Marouille et al. 2021; Paredes Bonilla et al. 2021). These computational models can be used to help predict the effect of different drug doses or treatment regimens (Frymoyer et al. 2019; Garcia-Cremades et al. 2019; Choi et al. 2021) and are helping to increase the pace of drug development, thereby getting new therapies to patients faster (Nayak et al. 2018). Computer simulation is also being used to help identify potential therapeutic compounds via in silico examination of drug candidates binding to target sites (de Witte et al. 2016; Bhardwaj and Purohit 2021). Not only can these molecular level simulations identify potentially useful compounds (Salo-Ahen et al. 2021;

Singh et al. 2021), but computer simulations of the binding process can help determine the residence time, thereby providing insight into potential drug side effects (Schuetz et al. 2017).

In this paper, we extend the use of mathematical modeling to the estimation of drug effectiveness parameters. We describe a new method, recently used to assess the effectiveness of quantum dot delivery of doxorubicin (Frieler et al. 2021), for determining time-independent values for IC_{50} and ϵ_{max} using mathematical model fitting to cell growth data. The objective of this study is to determine whether the new method can produce robust and reliable estimates, consistent with previous estimates from the literature, of both the IC_{50} and ϵ_{max} of doxorubicin in HeLa and MCF-7 cells. We measure growth of MCF-7 and HeLa cells both with and without doxorubicin for 14 days. We fit the experimental data with mathematical models to extract the ϵ_{max} and IC_{50} . While we find reasonable estimates for both values, we also observe that the parameters show some correlation and that ϵ_{max} is not always locally identifiable, suggesting that additional experimental measurements will be needed to ensure robust parameter estimation.

Methods

Experimental data

We chose to test the new methodology using two commonly-used cancer cell lines, MCF-7 (breast cancer cells) and HeLa (cervical cancer cells), treated with a common chemotherapy drug, doxorubicin (DOX). We opted to use two different cell lines to assess whether the method will work to estimate in IC_{50} and ϵ_{max} for different types of cancer. Doxorubicin is effective in slowing growth of a number of different types of cancer (Meredith and Dass 2016), adding to broader applicability of the method, if successful. Both MCF-7 and HeLa cell lines are known to respond to treatment with DOX and there are multiple estimates of the IC_{50} in both cell lines available in the literature (Amin et al. 2017; Alagumuthu and Arumugam 2017; Boraei et al. 2017; Kuete et al. 2016; Salem and Ali 2016; Attia et al. 2020; Robledo-Cadena et al. 2020; Andreeva et al. 2020; Phutdhawong et al. 2021; Gabr et al. 2016) to enable comparison with estimates determined with our new methodology.

MCF-7 and HeLa cells were obtained from ATCC (atcc.org). MCF-7 and HeLa cells were grown in cell culture using Dulbecco's modified eagle media (DMEM, 10% fetal bovine serum, 1% non-essential amino acids, L-glutamine, Penicillin, Streptomycin) at 37°C and 5% CO_2 . When cells reached confluency, the medium was aspirated and the cells were washed with 1x PBS. 0.05% trypsin was added to detach cells and was then quenched with DMEM. Cells were then

counted using a hemocytometer and plated and used in experiments with 10% of cells reserved in a new flask with DMEM.

The two cell lines were used in cell growth experiments where they were plated on 12 well trays at a density of 1,000 cells/well with 2 mL of medium in each well. The plates were incubated at 37°C and 5% CO₂. The chemotherapy drug doxorubicin was added at concentrations of 0.05, 0.005, 0.0005, and 0.00005 µg/mL. Measurements of cell growth were made every 48 h for 14 d. For each measurement, medium was removed from 3 of the wells and washed with 1x PBS. 0.05% trypsin was added to detach the cells and medium was added to quench the trypsin. Cells were then counted using a hemocytometer.

Mathematical modeling

Cancer growth is most commonly modeled with the logistic ordinary differential equation (ODE), so we use this as the basis for our parameter estimation (Verhulst 1838),

$$\frac{dN}{dt} = \lambda N \left(1 - \frac{N}{K}\right), \quad (1)$$

where N is the number of cancer cells, λ is the growth rate, and K is the carrying capacity. The logistic model produces a sigmoidal curve, meaning that the cell growth is limited by either space or access to nutrients.

We apply the effect of drug treatment in the models through the use of a drug efficacy parameter, ϵ . Drug efficacy is found from the applied drug concentration via the E_{\max} model (Holford and Sheiner 1981),

$$\epsilon = \epsilon_{\max} \frac{D}{IC_{50} + D}, \quad (2)$$

where D is the concentration of drug, ϵ_{\max} is the maximum effect of the drug, and IC_{50} is the drug concentration at which the drug achieves 50% of its maximum effect. When applying the drug effect we multiply a particular model parameter by $(1 - \epsilon)$ to cause a reduction in the value of the parameter. For example, multiplying λ in the logistic model by $(1 - \epsilon)$ will decrease the cell growth rate when drug is applied.

The anticancer drug doxorubicin disrupts DNA repair and generates free radicals that damage the cell membrane (Thorn et al. 2011; Sritharan and Sivalingam 2021), suggesting several possible mechanisms of action that need to be captured in the model. Thus we investigate different possible mechanisms of action by applying the drug effect to different parameters in the models. For the logistic model, we can apply the drug effect to the growth rate, indicating a drug that inhibits the cell replication rate in some capacity. A drug that is applied to the carrying capacity in the logistic

model could represent a drug that modulates host factors and the tumor environment (Mulder et al. 2019; Roskoski 2019; Awasthee et al. 2019).

Data fitting

We use a two-step fitting process. We first fit control data to determine the baseline parameters of the growth model. We then fit the treated cell growth data, using all drug doses simultaneously, to determine the IC_{50} and ϵ_{\max} . Fitting is done by minimizing the sum of squared residuals (SSR) using the Nelder-Mead algorithm implemented in Python. The initial number of cells is fixed to 1000 to match experimental protocol. We intentionally kept parameters within a biologically realistic range by using a logarithmic transformation on λ , K , and IC_{50} to ensure positive values and a logistic transformation on ϵ_{\max} in order for it to remain between 0 and 1. Goodness of fit was assessed both through SSR and through Akaike's "an information criterion" (AIC_C) for small sample size,

$$AIC_C = n \ln \left(\frac{SSR}{n} \right) + \frac{2(K+1)n}{n-K-2}, \quad (3)$$

where n is the number of data points and K is the number of parameters (Burnham and Anderson 2002). The model with the lowest AIC_C is considered to be the better model given the experimental data. 1000 bootstrap replicates were performed to determine 95% confidence intervals and assess parameter identifiability.

Results

Comparing drug mechanisms of action

Model fits to cell growth data of doxorubicin-treated MCF-7 and HeLa cells are shown in Fig. 1. Estimates for the best fit parameter values are given in Table 1. For MCF-7 cells, we find that the best model for describing the growth of treated MCF-7 cells, based on the lowest AIC_C value, is the logistic model with a drug effect applied to the carrying capacity, while for HeLa cells the assumption of a drug that reduces growth rate provides the better description. It is important to note, however, that the AIC_C of both drug models agree within error, so we essentially cannot distinguish between the two potential drug models.

For MCF-7 cells, we get IC_{50} values of 5.40×10^{-3} µg/mL (95% CI $(1.19-16.6) \times 10^{-3}$ µg/mL) for a drug that decreases growth rate and 1.86×10^{-3} µg/mL (95% CI, $(0.785-5.80) \times 10^{-3}$ µg/mL) for a drug that decreases carrying capacity, which are lower than IC_{50} estimates determined through traditional techniques that range from

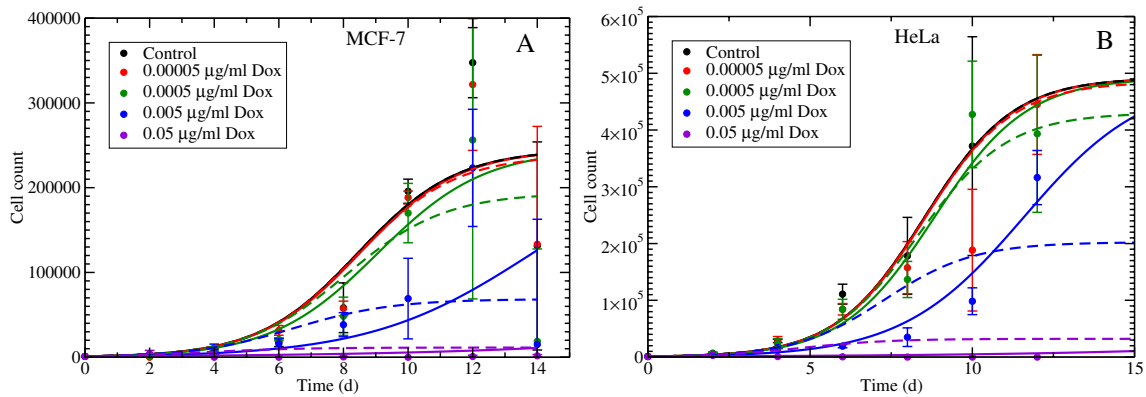


Fig. 1 Model fits to cell growth data treated with doxorubicin. Under the assumption of logistic growth, the solid lines give the best fit for a drug that acts on λ and the dashed lines give the best fit for a drug that acts on K for MCF-7 cells (**A**) and HeLa cells (**B**)

Table 1 Best fit parameter estimates for the logistic model under different drug mechanism assumptions

Drug effect	λ (/day)	K (cells)	IC_{50} ($\mu\text{g}/\text{mL}$)	ϵ_{\max}	SSR	AIC_C
MCF-7 cells						
Drug on λ	0.652	2.45×10^5	5.40×10^{-3}	0.813	1.38×10^{11}	890
95% Confidence interval	0.517–0.920	$(1.78–3.80) \times 10^5$	$(1.19–16.6) \times 10^{-3}$	0.445–1.00	$(0.366–2.31) \times 10^{11}$	837–911
Drug on K	0.652	2.45×10^5	1.86×10^{-3}	0.989	1.19×10^{11}	884
95% Confidence interval	0.517–0.920	$(1.78–3.80) \times 10^5$	$(0.785–5.80) \times 10^{-3}$	0.819–1.00	$(0.323–1.94) \times 10^{11}$	832–904
HeLa cells						
Drug on λ	0.727	4.92×10^5	0.0139	1.00	5.29×10^{10}	732
95% Confidence interval	0.655–0.767	$(3.86–7.87) \times 10^5$	0.00599–0.0391	0.418–1.00	$(0.920–11.5) \times 10^{10}$	679–758
Drug on K	0.727	4.92×10^5	3.48×10^{-3}	1.00	8.14×10^{10}	746
95% Confidence interval	0.655–0.767	$(3.86–7.87) \times 10^5$	$(1.68–22.9) \times 10^{-3}$	0.599–1.00	$(4.47–18.2) \times 10^{10}$	726–774

0.05–3.3 $\mu\text{g}/\text{mL}$ (Amin et al. 2017; Alagumuthu and Arumugam 2017; Boraie et al. 2017; Kuete et al. 2016; Salem and Ali 2016). The estimated maximum efficacy of the drug is high for both models — 0.813 (95% CI 0.445–1.00) and 0.989 (95% CI 0.819–1.00) — but does not hit the maximum allowed value of 1. For HeLa cells, the IC_{50} are of the same order of magnitude as for MCF-7 cells (13.9×10^{-3} $\mu\text{g}/\text{mL}$ (95% CI $(5.99–39.1) \times 10^{-3}$ $\mu\text{g}/\text{mL}$) for a drug that decreases growth rate and 3.48×10^{-3} $\mu\text{g}/\text{mL}$ (95% CI, $(1.68–22.9) \times 10^{-3}$ $\mu\text{g}/\text{mL}$) for a drug that decreases carrying capacity). These are also lower than IC_{50} estimates for doxorubicin in HeLa cells estimated via traditional methods, which range from 0.64–14 $\mu\text{g}/\text{mL}$ (Attia et al. 2020; Robledo-Cadena et al. 2020; Andreeva et al. 2020; Phutdhawong et al. 2021; Gabr et al. 2016). Reasons for these lower IC_{50} estimates in both cell lines are discussed in Sect. 3.4. The ϵ_{\max} estimates for HeLa cells are 1.00 for both models suggesting that there might be an issue with identifiability of this parameter.

Parameter identifiability

While model fitting will yield parameter estimates for IC_{50} and ϵ_{\max} , we would like to ensure that these parameters are uniquely identified. If there is insufficient data, then there are pairs of parameters that will yield similar curves. For example, in our case it might be possible to lower ϵ_{\max} , then lower the IC_{50} to compensate and still get the same SSR. Since these parameters are used to help determine dosages in treatment, it is important that we ensure such a trade-off is not happening. Figure 2 shows the parameter correlation plots for logistic model fits to the MCF-7 data (top row) and the HeLa cell data (bottom row). Ideally, the correlation plots should be scattered points in a circle, indicating no clear relationship between the two parameters. In this case, there appear to be relationships between the parameters. When fitting the control data, lower growth rates require higher carrying capacities in order to fit the data well. For the drug effectiveness parameters, we see a tendency of

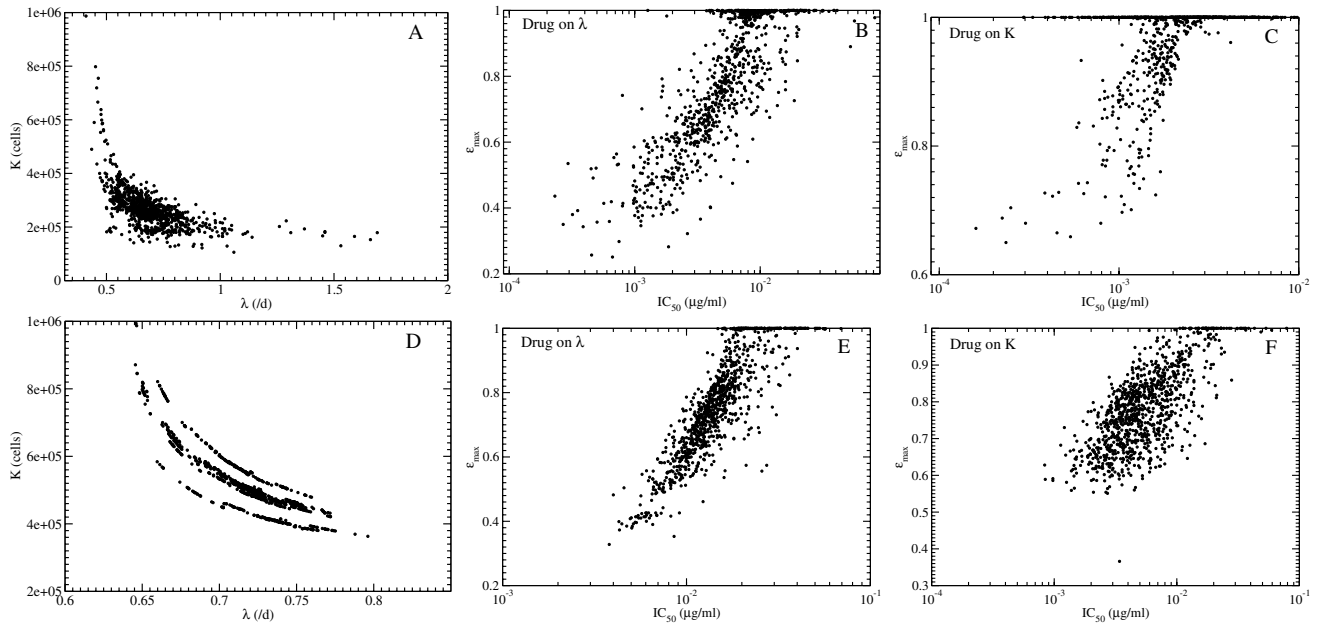


Fig. 2 Correlation plots for parameter estimates of logistic model fits to MCF-7 and HeLa data. We plot the results of parameter estimates from 1000 bootstrap replicates for **A** and **D** λ and K , **B**, **E** IC_{50} and

ϵ_{max} for drug effect on λ , and **C**, **F** IC_{50} and ϵ_{max} for drug effect on K for MCF-7 cells (top row) and HeLa cells (bottom row)

ϵ_{max} to be at its maximum value of 1. When ϵ_{max} moves off this value, there appears to be a correlation between ϵ_{max} and IC_{50} where lower values of ϵ_{max} result in lower values of IC_{50} .

The tendency of ϵ_{max} to be at its maximum value of 1 suggests that there might be difficulty in reaching a minimum of the SSR. To investigate this possibility, we examined the likelihood profiles. These are shown for the fits of the logistic model to MCF-7 cells in Fig. 3 and for HeLa cells in Fig. 4. The likelihood profiles are all parabolic, with our estimated best fit value at the minimum, with the exception of the ϵ_{max} estimate for HeLa cells under the assumption of a drug that reduces carrying capacity. The likelihood profile near that estimate of ϵ_{max} is also parabolic, but the minimum is reached at values of ϵ_{max} higher than 1. With the exception of that one estimate of ϵ_{max} , the profiles indicate that there is at least local identifiability of the parameters (Raue et al. 2009).

Additional measurements

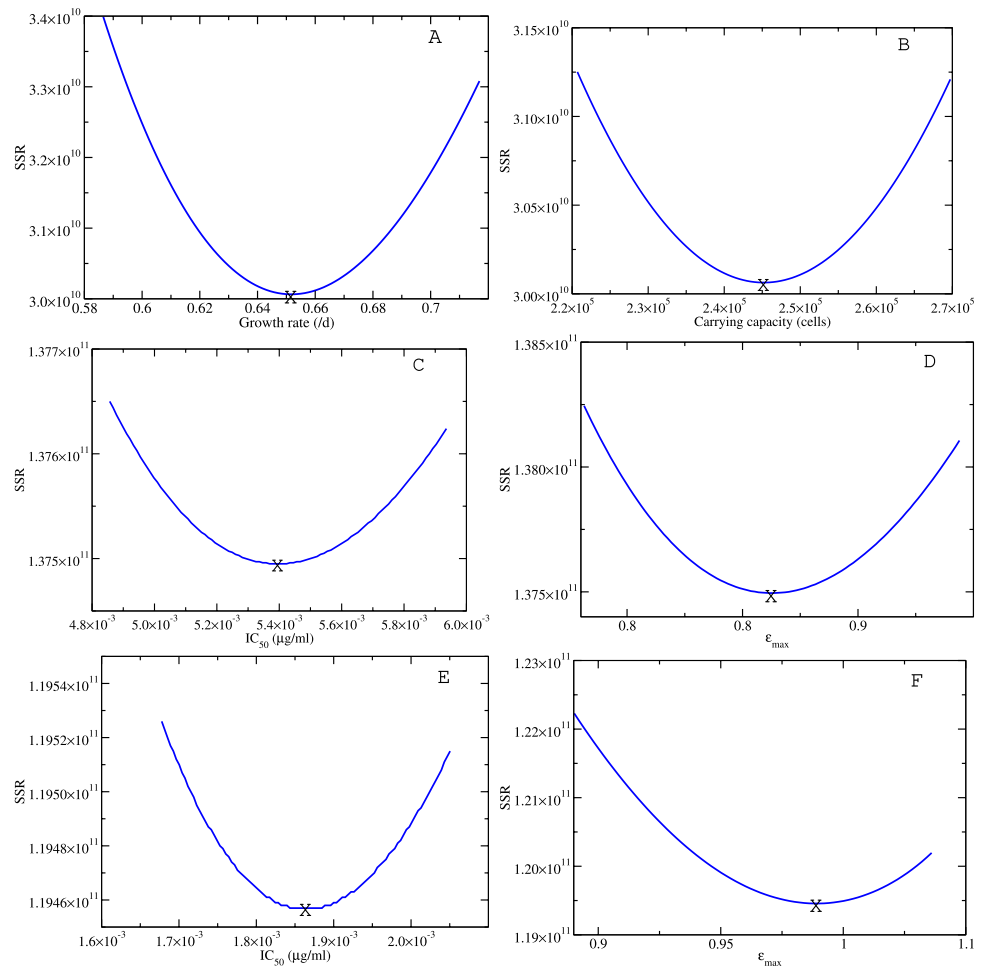
While the likelihood profiles show that most of the parameters are locally identifiable, the correlations between IC_{50} and ϵ_{max} suggest that we should explore the possibility of additional experimental measurements that might help refine the parameter estimates. We performed additional experiments using MCF-7 cells with two additional drug doses between 0.005–0.0005 $\mu\text{g}/\text{mL}$. We chose additional doses in this range because there is a gap between curves

in this range, so additional measurements here might help better define the dose response and lead to better estimates of IC_{50} and ϵ_{max} .

We fit the extended data set using the logistic model and both options for modeling of the drug effect. The model fits to experimental data, along with correlation plots and likelihood profiles, are shown in Fig. 5. Fig. 5 shows the model fits to the extended data set (note the two additional lines for treatment with DOX at concentrations of 0.01 $\mu\text{g}/\text{mL}$ and 0.015 $\mu\text{g}/\text{mL}$). While the correlation plots and likelihood profiles look similar to those generated from the original data set, we do find some slight differences. The correlation plots show less clustering near the maximum ϵ_{max} value of 1, however, the ϵ_{max} is no longer at the minimum of the likelihood profile for either drug mechanism.

Note that the control data is the same for our original and extended data sets, and since we use a two-step fitting process, the growth rate and carrying capacity estimated values are the same as in Table 1, so only the new IC_{50} and ϵ_{max} estimates are given in Table 2. While the IC_{50} values found for the extended data set are not exactly the same as for the original data, they do agree within error indicating some robustness in the IC_{50} estimate. The ϵ_{max} values for both drug assumptions are estimated to be the maximum value of 1.0. Interestingly, the AIC_C for both drug assumptions is basically the same, again suggesting an inability to pinpoint drug mechanism of action in this simple cancer growth model.

Fig. 3 Likelihood profiles for the parameter estimates of the logistic model fits to MCF-7 cell growth data. Figures show the changes in SSR as the following parameters are varied about their best fit estimate: **A** λ , **B** K , **C** IC_{50} for a drug effect on λ , **D** ϵ_{max} for a drug effect on λ , **E** IC_{50} for a drug effect on K , **F** ϵ_{max} for a drug effect on K . X marks the position of the best fit estimate



The additional experimental measurements did not help break the correlation between IC_{50} and ϵ_{max} estimates. While we have maintained identifiability of IC_{50} values for both models, unfortunately we are no longer able to identify ϵ_{max} for either model. The local minimum of the SSR occurs at values of ϵ_{max} higher than 1 for both drug assumptions. The additional experimental measurements did not help reduce the uncertainty in parameter estimates or improve parameter identifiability.

Traditional IC_{50} estimates

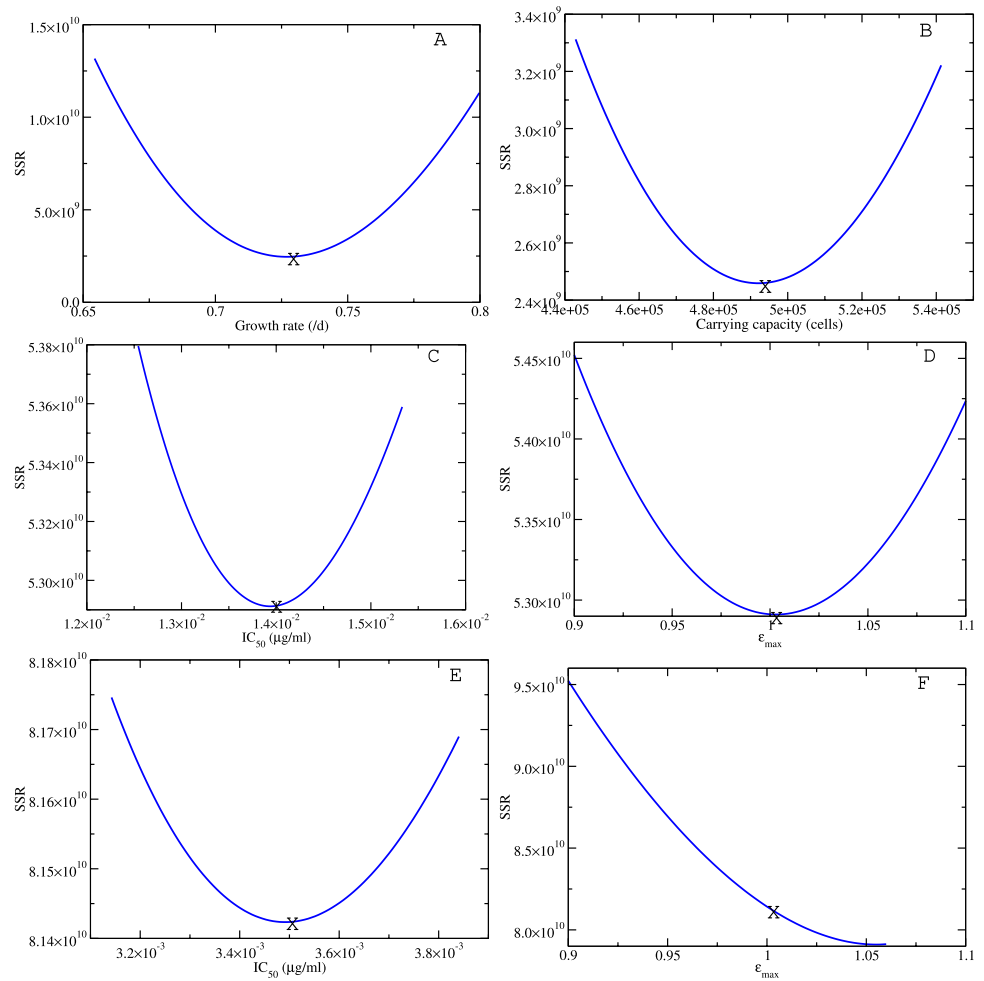
We used the parameter estimates from Table 1 and the mathematical model to simulate traditional dose–response curves for each of the parameter sets. Cell cultures were initiated with 5000 cells and cells were counted 48 h after application of a particular concentration of doxorubicin. Dose–response curves are shown in Fig. 6. IC_{50} and ϵ_{max} measurements derived from the dose response curves are given in the table. We can see that estimation of IC_{50} and ϵ_{max} using dose response curves derived from cell viability at a specific time leads to an IC_{50} estimate different from the IC_{50} used for

simulation. In particular, the IC_{50} measured via cell viability underestimates the true IC_{50} when we assume a drug acts on growth rate and overestimates the true IC_{50} when we assume a drug acts on carrying capacity. This example shows the distinction that needs to be made between an IC_{50} that represents a drug’s effect on cell viability and an IC_{50} that represents a drug’s effect on a particular biological process.

Discussion

In this study, we used in vitro cell growth data to estimate two parameters, IC_{50} and ϵ_{max} , that characterize the efficacy of doxorubicin in MCF-7 and HeLa cell lines. For MCF-7 cells, we found that the effect of doxorubicin was better described by reduction in the carrying capacity, while for HeLa cells, the effect of doxorubicin was better described by reduction in the growth rate. Doxorubicin is known to have a number of different effects on cells (Thorn et al. 2011; Sritharan and Sivalingam 2021), including causing damage to cell DNA by disrupting topoisomerase-II (TOP2)-mediated DNA repair. Doxorubicin is also known to generate

Fig. 4 Likelihood profiles for the parameter estimates of the logistic model fits to HeLa cell growth data. Figures show the changes in SSR as the following parameters are varied about their best fit estimate: **A** λ , **B** K , **C** IC_{50} for a drug effect on λ , **D** ϵ_{max} for a drug effect on λ , **E** IC_{50} for a drug effect on K , **F** ϵ_{max} for a drug effect on K . X marks the position of the best fit estimate



free radicals that can cause damage to the cell membrane. Neither of these mechanisms can be explicitly incorporated in the logistic model since the model lacks biological detail, so it is likely the effect of the drug is captured to some extent by both drug model formulations. Experiments have noted some differences in response of MCF-7 and HeLa cell lines to doxorubicin (Khan et al. 2018; Kazan et al. 2020), so which mathematical model best captures the effect of doxorubicin will depend on which mechanism dominates in a particular cell line.

We found that the IC_{50} estimates using our new method were lower than IC_{50} estimates found in the literature for doxorubicin treatment of both cell lines. Traditional estimates of IC_{50} assess cell viability at a particular measurement time and are known to be dependent on the specific time chosen to assess cell viability (Murphy et al. 2020; Harris et al. 2016; Hafner et al. 2016). Thus, traditional IC_{50} measurements are an indication of how the drug affects cell viability at a specific time, whereas the IC_{50} estimate produced by our technique is an indication of how the drug alters a particular biological process: either change in growth rate or carrying capacity in this case.

Previous work has shown that traditional IC_{50} measurements underestimate the mechanistic IC_{50} when we assume a drug acts on growth rate and overestimate the mechanistic IC_{50} when we assume a drug acts on carrying capacity (Murphy et al. 2020), as we saw when we used our parameter estimates to simulate cell viability assays.

While this method allows for estimation of IC_{50} and ϵ_{max} that are independent of measurement time and are more representative of drug mechanism, there are still problems that need to be resolved. We found that with a 14 day time course, we were unable to uniquely identify the parameters. There were correlations between the carrying capacity and growth rate estimates for the logistic model, although we reached a local minimum SSR for both parameters. The IC_{50} was also always locally identifiable, but ϵ_{max} tended towards its maximum possible value and often was not at a local minimum. We attempted to address this issue by adding additional experimental measurements at intermediate drug concentrations, but this did not fix the problem. Further work to address this might involve more frequent measurements or measurement of cell growth

Fig. 5 Model fits to extended MCF-7 cell growth data treated with doxorubicin. **A** Under the assumption of logistic growth, the solid lines give the best fit for a drug that acts on λ and the dashed lines give the best fit for a drug that acts on K . Correlation plots for IC_{50} and ϵ_{max} estimates assuming doxorubicin decreases growth rate (**B**) and assuming doxorubicin decreases carrying capacity (**C**). Likelihood profiles for IC_{50} (**D**) and ϵ_{max} (**E**) under the assumption that doxorubicin decreases growth rate. Likelihood profiles for IC_{50} (**F**) and ϵ_{max} (**G**) under the assumption that doxorubicin decreases carrying capacity

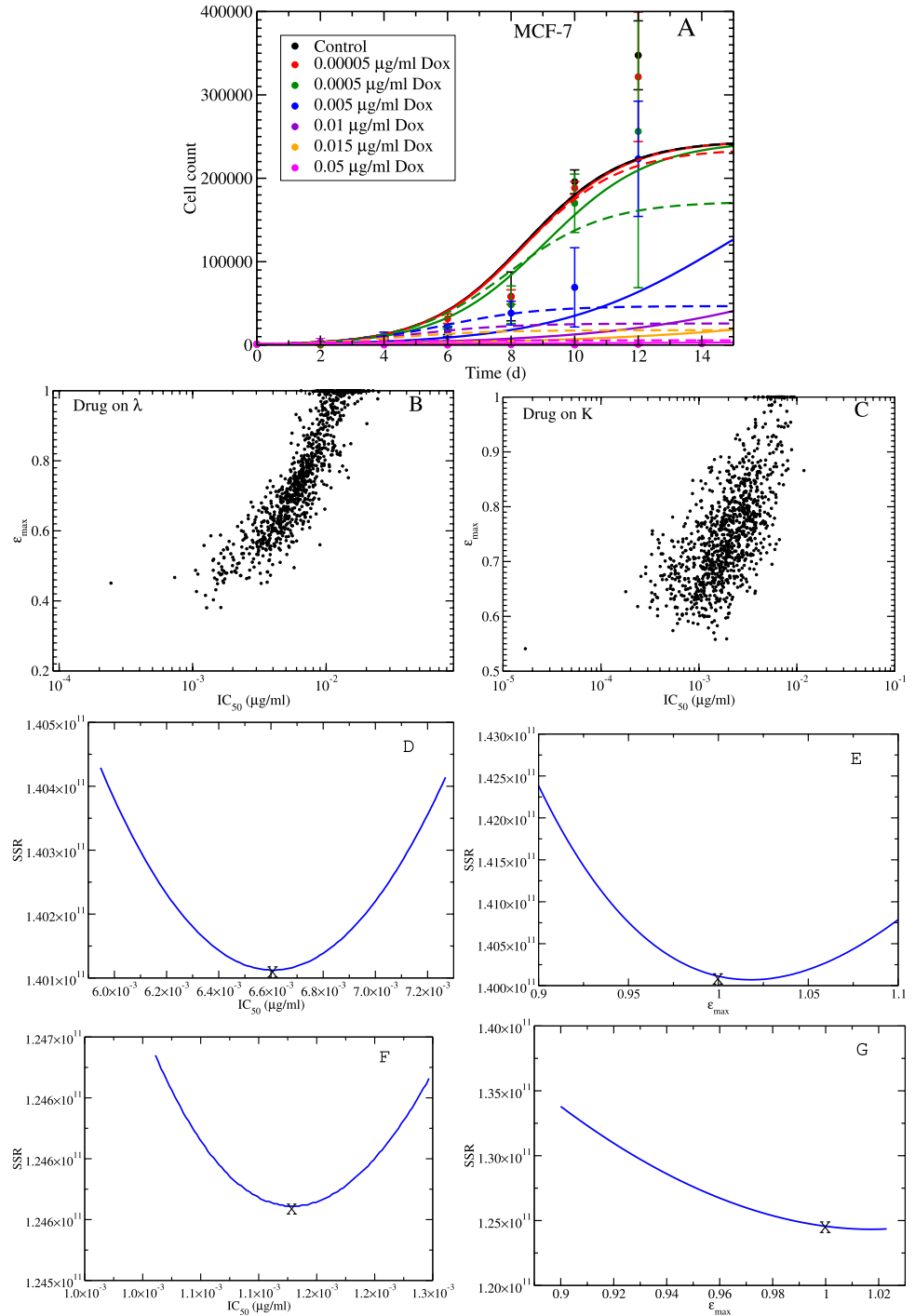
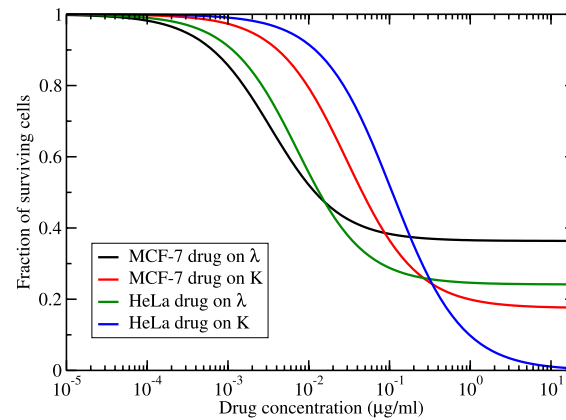


Table 2 Best fit parameter estimates for the extended MCF-7 data set with the logistic model

Drug effect	IC_{50} ($\mu\text{g/mL}$)	ϵ_{max}	SSR	AIC_C
Drug on λ	6.61×10^{-3}	1.00	1.40×10^{11}	1220
95% Confidence interval	$(1.66-16.5) \times 10^{-3}$	0.479-1.00	$(0.366-2.25) \times 10^{11}$	1150-1250
Drug on K	1.18×10^{-3}	1.00	1.25×10^{11}	1220
95% Confidence interval	$(0.411-6.94) \times 10^{-3}$	0.604-1.00	$(0.552-1.90) \times 10^{11}$	1170-1240

Fig. 6 Simulated dose response curves for MCF-7 and HeLa cells under different drug mechanism of action assumptions. Parameters for the simulations are given in Table 1. Simulations are initiated with 5000 cells and measurements are made after 48 h. IC_{50} and ϵ_{max} estimated by fitting the dose response curve are given in the table



Curve	IC_{50} ($\mu\text{g/mL}$) (actual)	IC_{50} ($\mu\text{g/mL}$) (measured)	ϵ_{max} (actual)	ϵ_{max} (measured)
MCF-7 drug on λ	5.40×10^{-3}	3.37×10^{-3}	0.813	0.637
MCF-7 drug on K	1.86×10^{-3}	3.00×10^{-3}	0.989	0.825
HeLa drug on λ	13.9×10^{-3}	7.17×10^{-3}	1.00	0.760
HeLa drug on K	3.48×10^{-3}	108×10^{-3}	1.00	1.00

over a longer period of time, which, however, does not guarantee a universal fix of the issue.

Another potential route to address the identifiability problem is to use alternative mathematical models of cancer growth. There are several simple ordinary differential equation models used to describe cancer growth (Gerlee 2013; Murphy et al. 2016; Sharpe and Dobrovoly 2021) and many mathematical models that include more details of the cancer growth process (Abbas-Aghababazadeh et al. 2019; Brady and Enderling 2019). Since the logistic model used in this work only has two parameters, each parameter represents a number of different underlying biological processes, only some of which might be affected by the drug. This lack of detail could be limiting our ability to select a best mathematical representation of the effect of doxorubicin. This could also be contributing to the limited identifiability of ϵ_{max} and the correlation between ϵ_{max} and IC_{50} . However, even more detailed models have noted similar problems in fitting experimental cancer growth data. A study assessing the effect of androgen suppression therapy on prostate cancer noted difficulty in determining many of the parameters of their model (Wu et al. 2019). A detailed study of the identifiability of a different cancer growth model suggests that lack of practical identifiability could lead to incorrect treatment efficacy estimates (Eisenberg and Jain 2017). More generally, researchers are trying to devise criteria for both models and data that would allow separation of drug efficacy parameters and system parameters (Evans et al. 2018) or are investigating alternative fitting methods that might lead to better parameter identifiability (Rutter et al. 2009; Chrysanthopoulou et al. 2021; Keroui et al. 2020).

Conclusion

This new joint theoretical and experimental study presents a preliminary assessment of model fitting of *in vitro* cancer growth data as a means of estimating the drug efficacy parameters IC_{50} and ϵ_{max} . The method shows promise in being able to provide an estimate of IC_{50} that is independent of measurement time and more closely linked to the mechanism of action of the drug, which was not previously achieved. The limitations of the study are that parameter identifiability and robustness of the parameter estimates have not been established. Future studies are needed to assess whether more frequent measurements, longer time courses, or growth model choice will improve the reliability of this method.

Acknowledgements This research was funded by TCU Invests in Scholarship grant (Hana Dobrovoly).

Author contributions Conceptualization: HMD, GRA and AVN; Data curation: MF, CP and HMD; Formal analysis: MF, CP and HMD; Investigation: MF, CP, and HD; Project administration: HMD; Resources: HMD, GRA and AVN; Supervision: HMD, GRA and AVN; Visualization: MF, CP, and HMD; Writing—original draft: CP; Writing—review and editing: HMD, GRA and AVN. All authors have read and agreed to the published version of the manuscript.

Availability of data and materials All data is included in the manuscript and supplementary material.

Code availability Data fitting codes are available in the github repository hdrobrovo/Cancer_fitting.

Declarations

Funding This research was funded by TCU Invests in Scholarship grant (Hana Dobrovolny).

Conflict of interest The authors have no conflicts of interest to declare.

Ethics approval Not applicable.

Consent to participate Not applicable.

Consent for publication Not applicable.

References

- Abbas-Aghababazadeh F, Lu P, Fridley BL (2019) Nonlinear mixed-effects models for modeling in vitro drug response data to determine problematic cancer cell lines. *Sci Rep* 9:14421. <https://doi.org/10.1038/s41598-019-50936-0>
- Alagumuthu M, Arumugam S (2017) Molecular explorations of substituted 2-(4-phenylquinolin-2-yl) phenols as phosphoinositide 3-kinase inhibitors and anticancer agents. *Cancer Chemother Pharmacol* 79(2):389–397
- Amin KM, Syam YM, Anwar MM, Ali HI, Abdel-Ghani TM, Serry AM (2017) Synthesis and molecular docking studies of new furochromone derivatives as p38alpha MAPK inhibitors targeting human breast cancer MCF-7 cells. *Bioorg Med Chem* 25(8):2423–2436. <https://doi.org/10.1016/j.bmc.2017.02.065>
- Andreeva OV, Garifullin BF, Sharipova RR, Strobkykina IY, Sapunova AS, Voloshina AD, Belenok MG, Dobrynin AB, Khabibulina LR, Kataev VE (2020) Glycosides and glycoconjugates of the diterpenoid isosteviol with a 1,2,3-triazolyl moiety: Synthesis and cytotoxicity evaluation. *J Nat Prod* 83(8):2367–2380. <https://doi.org/10.1021/acs.jnatprod.0c00134>
- Attia MH, Elrazaz EZ, El-Emam SZ, Taher AT, Abdel-Aziz HA, Abouzid KAM (2020) Synthesis and in-vitro anti-proliferative evaluation of some pyrazolo [1,5-a]pyrimidines as novel larotrectinib analogs. *Bioorg Chem* 94:103458. <https://doi.org/10.1016/j.bioorg.2019.103458>
- Awasthee N, Rai V, Chava S, Nallasamy P, Kunnumakkara AB, Bishayee A, Chauhan SC, Challagundla KB, Gupta SC (2019) Targeting I kappa appaB kinases for cancer therapy. *Sem Cancer Biol* 56:12–24. <https://doi.org/10.1016/j.semcancer.2018.02.007>
- Bae SY, Guan N, Yan R, Warner K, Taylor SD, Meyer AS (2020) Measurement and models accounting for cell death capture hidden variation in compound response. *Cell Death Dis* 11(4):255. <https://doi.org/10.1038/s41419-020-2462-8>
- Bhardwaj VK, Purohit R (2021) Targeting the protein-protein interface pocket of Aurora-A-TPX2 complex: rational drug design and validation. *J Biomol Struct Dyn* 39(11):3882–3891. <https://doi.org/10.1080/07391102.2020.1772109>
- Boraei ATA, Gomaa MS, El Ashry ESH, Duerkop A (2017) Design, selective alkylation and X-ray crystal structure determination of dihydro-indolyl-1,2,4-triazole-3-thione and its 3-benzylsulfanyl analogue as potent anticancer agents. *Eur J Med Chem* 125:360–371. <https://doi.org/10.1016/j.ejmech.2016.09.046>
- Brady R, Enderling H (2019) Mathematical models of cancer: when to predict novel therapies, and when not to. *Bull Math Biol* 81(10):3722–3731. <https://doi.org/10.1007/s11538-019-00640-x>
- Bray F, Ferlay J, Soerjomataram I, Siegel RL, Torre LA, Jemal A (2018) Global cancer statistics 2018 Globocan estimates of incidence and mortality worldwide for 36 cancers in 185 countries. *CA* 68(6):394–424. <https://doi.org/10.3322/caac.21492>
- Brooks EA, Galarza S, Gencoglu MF, Cornelison RC, Munson JM, Peyton SR (2019) Applicability of drug response metrics for cancer studies using biomaterials. *Philos Trans R Soc B* 374(1779):20180226. <https://doi.org/10.1098/rstb.2018.0226>
- Burnham KP, Anderson DR (2002) Model selection and multimodel inference: a practical information-theoretic approach, 2nd edn. Springer, New York
- Calhelha RC, Martínez MA, Isabel MAP, Ferreira CFR (2017) Mathematical models of cytotoxic effects in endpoint tumor cell line assays: critical assessment of the application of a single parametric value as a standard criterion to quantify the dose-response effects and new unexplored proposal formats. *Analyst* 142:4124–4141. <https://doi.org/10.1039/c7an00782e>
- Chen B, Dong JQ, Pan W-J, Ruiz A (2012) Pharmacokinetics/pharmacodynamics model-supported early drug development. *Curr Pharm Biotechnol* 13(7):1360–1375. <https://doi.org/10.2174/138920112800624436>
- Choi YH, Zhang C, Liu Z, Tu M-J, Yu A-X, Yu A-M (2021) A novel integrated pharmacokinetic-pharmacodynamic model to evaluate combination therapy and determine in vivo synergisms. *J Pharmacol Exp Ther* 377(3):305–315. <https://doi.org/10.1124/jpet.121.000584>
- Chrysanthopoulou SA, Rutter CM, Gatsonis CA (2021) Bayesian versus empirical calibration of microsimulation models: a comparative analysis. *Med Dec Making* 41(6):714–726. <https://doi.org/10.1177/0272989X211009161>
- de Witte WEA, Wong YC, Nederpelt I, Heitman LH, Danhof M, van der Graaf PH, Gilissen RAHJ, de Lange ECM (2016) Mechanistic models enable the rational use of in vitro drug-target binding kinetics for better drug effects in patients. *Exp Opin Drug Discov* 11(1):45–63. <https://doi.org/10.1517/17460441.2016.1100163>
- Eisenberg MC, Jain HV (2017) A confidence building exercise in data and identifiability: modeling cancer chemotherapy as a case study. *J Theor Biol* 437:63–78. <https://doi.org/10.1016/j.jtbi.2017.07.018>
- Evans ND, Cheung SYA, Yates JWT (2018) Structural identifiability for mathematical pharmacology: models of myelosuppression. *J Pharmacokin Pharmacodyn* 45(1):79–90. <https://doi.org/10.1007/s10928-018-9569-x>
- Fallahi-Sichani M, Honarnejad S, Heiser LM, Gray JW (2013) Metrics other than potency reveal systematic variation in responses to cancer drugs. *Nat Chem Biol* 9(11):708. <https://doi.org/10.1038/NCHEMBO.1337>
- Frieler M, Pho C, Lee B, Dobrovolny HM, Naumov A, Akkaraju G (2021) Effects of doxorubicin delivery by nitrogen-doped graphene quantum dots on cancer cell growth: experimental study and mathematical modeling. *Nanomaterials* 11:140. <https://doi.org/10.3390/nano11010140>
- Frymoyer A, Stockmann C, Hersh AL, Goswami S, Keizer RJ (2019) Individualized empiric vancomycin dosing in neonates using a model-based approach. *J Ped Infect Dis Soc* 8(2):97–104. <https://doi.org/10.1093/jpids/pix109>
- Gabr MT, El-Gohary NS, El-Bendary ER, El-Kerdawy MM, Ni N (2016) Synthesis, in vitro antitumor activity and molecular modeling studies of a new series of benzothiazole Schiff bases. *Chin Chem Lett* 27(3):380–386. <https://doi.org/10.1016/j.ccl.2015.12.033>
- Garcia-Cremades M, Pitou C, Iversen PW, Troconiz IF (2019) Translational framework predicting tumour response in gemcitabine-treated patients with advanced pancreatic and ovarian cancer from xenograft studies. *AAPS J* 21(2):23. <https://doi.org/10.1208/s12248-018-0291-9>
- Gerlee P (2013) The model muddle: in search of tumor growth laws. *Cancer Res* 73(8):2407–2411. <https://doi.org/10.1158/0008-5472.CAN-12-4355>

- Gupta A, Gautam P, Wennerberg K, Aittokallio T (2020) A normalized drug response metric improves accuracy and consistency of anticancer drug sensitivity quantification in cell-based screening. *Commun Biol* 3(1):42. <https://doi.org/10.1038/s42003-020-0765-z>
- Gurney H (2002) How to calculate the dose of chemotherapy. *Br J Cancer* 86(8):1297–1302. <https://doi.org/10.1038/sj.bjc.6600139>
- Hafner M, Niepel M, Chung M, Sorger PK (2016) Growth rate inhibition metrics correct for confounders in measuring sensitivity to cancer drugs. *Nat Methods* 13(6):521. <https://doi.org/10.1038/NMETH.3853>
- Harris LA, Frick PL, Garbett SP, Hardeman KN, Paudel BB, Lopez CF, Quaranta V, Tyson DR (2016) An unbiased metric of anti-proliferative drug effect in vitro. *Nat Methods* 13(6):497–502. <https://doi.org/10.1038/nMeth.3852>
- Holford NHG, Sheiner LB (1981) Understanding the dose-effect relationship: Clinical application of pharmacokinetic-pharmacodynamic models. *Clin Pharmacokinet* 6(6):429–453
- Kazan HH, Urfali-Mamatoglu C, Yalcin GD, Bulut O, Sezer A, Banerjee S, Gunduz U (2020) 15-LOX-1 has diverse roles in the resensitization of resistant cancer cell lines to doxorubicin. *J Cell Physiol* 235(5):4965–4978. <https://doi.org/10.1002/jcp.29375>
- Kerroum M, Mercier F, Bertrand J, Tardivon C, Bruno R, Guedj J, Desmees S (2020) Bayesian inference using Hamiltonian Monte-Carlo algorithm for nonlinear joint modeling in the context of cancer immunotherapy. *Stat Med* 39(30):4853–4868. <https://doi.org/10.1002/sim.8756>
- Khan AU, Khan M, Cho MH, Khan MM (2020) Optimization of chemotherapy and immunotherapy: in silico analysis using pharmacokinetic-pharmacodynamic and tumor growth models. *Bioprocess Biosys Eng*. <https://doi.org/10.1007/s00449-020-02330-8>
- Khan FM, Saleh E, Alawadhi H, Harati R, Zimmermann W-H, El-Awady R (2018) Inhibition of exosome release by ketotifen enhances sensitivity of cancer cells to doxorubicin. *Cancer Biol Ther* 19(1):25–33. <https://doi.org/10.1080/15384047.2017.1394544>
- Kuete V, Omosa LK, Tala VRS, Midiwo JO, Mbaveng AT, Swaleh S, Karaosmanoglu O, Sivas H (2016) Cytotoxicity of plumbagin, rapanone and 12 other naturally occurring quinones from kenyan flora towards human carcinoma cells. *BMC Pharmacol Toxicol* 17:60. <https://doi.org/10.1186/s40360-016-0104-7>
- Kurilov R, Haibe-Kains B, Brors B (2020) Assessment of modelling strategies for drug response prediction in cell lines and xenografts. *Sci Rep* 10(1):2849. <https://doi.org/10.1038/s41598-020-59656-2>
- Larsson P, Engqvist H, Biermann J, Ronnerman EW, Forssell-Aronsson E, Kovacs A, Karlsson P, Helou K, Parris TZ (2020) Optimization of cell viability assays to improve replicability and reproducibility of cancer drug sensitivity screens. *Sci Rep* 10(1):5798. <https://doi.org/10.1038/s41598-020-62848-5>
- Marouille AL, Petit E, Kaderbhai C, Desmoulins I, Hennequin A, Mayeur D, Fumet J-D, Ladoire S, Tharin Z, Ayati S, Royer Ilie S, Schmitt AB (2021) Pharmacokinetic/pharmacodynamic model of neutropenia in real-life palbociclib-treated patients. *Pharmaceutics*. <https://doi.org/10.3390/pharmaceutics13101708>
- Meredith A-M, Dass CR (2016) Increasing role of the cancer chemotherapeutic doxorubicin in cellular metabolism. *J Pharm Pharmacol* 68(6):729–741. <https://doi.org/10.1111/jphp.12539>
- Miller KD, Siegel RL, Lin CC, Mariotto AB, Kramer JL, Rowland JH, Stein KD, Alteri R, Jemal A (2016) Cancer treatment and survivorship statistics, 2016. *Cancer J Clin* 66(4):271–289. <https://doi.org/10.3322/caac.21349>
- Mulder WJM, Ochando J, Joosten LAB, Fayad ZA, Netea MG (2019) Therapeutic targeting of trained immunity. *Nat Rev Drug Discov* 18(7):553–566. <https://doi.org/10.1038/s41573-019-0025-4>
- Murphy H, McCarthy G, Dobrovolny HM (2016) Differences in predictions of ode models of tumor growth: a cautionary example. *BMC Cancer* 16:163. <https://doi.org/10.1186/s12885-016-2164-x>
- Murphy H, Jaafari H, Dobrovolny HM (2020) Understanding the effect of measurement time on drug characterization. *Plos One* 15(5):0233031. <https://doi.org/10.1371/journal.pone.0233031>
- Nayak S, Sander O, Al-Huniti N, de Alwis D, Chain A, Chenel M, Sunkaraneni S, Agrawal S, Gupta N, Visser SAG (2018) Getting innovative therapies faster to patients at the right dose: Impact of quantitative pharmacology towards first registration and expanding therapeutic use. *Clin. Pharmacol. Therapeut.* 103(3):378–383. <https://doi.org/10.1002/cpt.978>
- Niepel M, Hafner M, Mills CE, Subramanian K, Williams EH, Chung M, Gaudio B, Barrette AM, Stern AD, Hu B, Korkola JE, Gray JW, Birtwistle MR, Heiser LM, Sorger PK, Shamu CE, Jayaraman G, Azeloglu EU, Iyengar R, Sobie EA, Mills GB, Liby T, Jaffe JD, Alimova M, Davison D, Lu X, Golub TR, Subramanian A, Shelley B, Svendsen CN, Ma'ayan A, Medvedovic M (2019) A multi-center study on the reproducibility of drug-response assays in mammalian cell lines. *Cell Syst* 9(1):35. <https://doi.org/10.1016/j.cels.2019.06.005>
- Paredes Bonilla RV, Nekka F, Craig M (2021) Therapy burden, drug resistance, and optimal treatment regimen for cancer chemotherapy. *Pharmacology* 106(9–10):542–550. <https://doi.org/10.1159/000518037>
- Peng T, Deng Z, He J, Li Y, Tan Y, Peng Y, Wang X-Q, Tan W (2020) Functional nucleic acids for cancer theranostics. *Coord. Chem. Rev.* 403:213080. <https://doi.org/10.1016/j.ccr.2019.213080>
- Phutdhawong W, Chuenchid A, Taechowisan T, Sirirak J, Phutdhawong WS (2021) Synthesis and biological activity evaluation of coumarin-3-carboxamide derivatives. *Molecules* 26(6):1653. <https://doi.org/10.3390/molecules26061653>
- Raue A, Kreutz C, Maiwald T, Bachmann J, Schilling M, Klingmüller U, Timmer J (2009) Structural and practical identifiability analysis of partially observed dynamical models by exploiting the profile likelihood. *Bioinformatics* 25(15):1923–1929
- Rejinold NS, Choi G, Choy J-H (2020) Recent trends in nano photochemo therapy approaches and future scopes. *Coord Chem Rev* 411:213252. <https://doi.org/10.1016/j.ccr.2020.213252>
- Robledo-Cadena DX, Gallardo-Perez JC, Davila-Borja V, Pacheco-Velazquez SC, Belmont-Diaz JA, Ralph SJ, Blanco-Carpintero BA, Moreno-Sanchez R, Rodriguez-Enriquez S (2020) Non-steroidal anti-inflammatory drugs increase cisplatin, paclitaxel, and doxorubicin efficacy against human cervix cancer cells. *Pharmaceutics* 13(12):463. <https://doi.org/10.3390/ph13120463>
- Roskoski R (2019) Properties of FDA-approved small molecule protein kinase inhibitors. *Pharm Res* 144:19–50. <https://doi.org/10.1016/j.phrs.2019.03.006>
- Rutter CM, Miglioretti DL, Savarino JE (2009) Bayesian calibration of microsimulation models. *J Am Stat Assoc* 104(488):1338–1350. <https://doi.org/10.1198/jasa.2009.ap07466>
- Salem MS, Ali MAM (2016) Novel pyrazolo[3,4-b]pyridine derivatives: Synthesis, characterization, antimicrobial and antiproliferative profile. *Biol Pharmaceut Bull* 39(4):473–483
- Salo-Ahen OMH, Alanko I, Bhadane R, Bonvin AMJJ, Honorato RV, Hossain S, Juffer AH, Kabelev A, Lahtela-Kakkonen M, Larsen AS, Lescrinier E, Marimuthu P, Mirza MU, Mustafa G, Nunes-Alves A, Pansar T, Saadabadi A, Singaravelu K (2021) Molecular dynamics simulations in drug discovery and pharmaceutical development. *Processes* 9(1):71. <https://doi.org/10.3390/pr9010071>
- Schuetz DA, de Witte WEA, Wong YC, Knasmueller B, Richter L, Kokh DB, Sadiq SK, Bosma R, Nederpelt I, Heitman LH, Segala E, Amaral M, Guo D, Andres D, Georgi V, Stoddart LA, Hill S, Cooke RM, De Graaf C, Leurs R, Frech M, Wade RC (2017) Kinetics for drug discovery: an industry-driven effort to target

- drug residence time. *Drug Discov Today* 22(6):896–911. <https://doi.org/10.1016/j.drudis.2017.02.002>
- Sharpe S, Dobrovolny HM (2021) Predicting the effectiveness of chemotherapy using stochastic ODE models of tumor growth. *Commun Nonlinear Sci Numer Simul* 101:105883. <https://doi.org/10.1016/j.cnsns.2021.105883>
- Singh R, Bhardwaj VK, Sharma J, Das P, Purohit R (2021) Identification of selective cyclin-dependent kinase 2 inhibitor from the library of pyrrolone-fused benzosuberene compounds: an in silico exploration. *J Biomol Struct Dyn* 318:1–9. <https://doi.org/10.1080/07391102.2021.1900918>
- Sritharan S, Sivalingam N (2021) A comprehensive review on time-tested anticancer drug doxorubicin. *Life Sci* 278:119527. <https://doi.org/10.1016/j.lfs.2021.119527>
- Tang W, Zhao G (2020) Small molecules targeting HIF-1 alpha pathway for cancer therapy in recent years. *Bioorg Mol Chem* 28(2):115235. <https://doi.org/10.1016/j.bmc.2019.115235>
- Thorn CF, Oshiro C, Marsh S, Hernandez-Boussard T, McLeod H, Klein TE, Altman RB (2011) Doxorubicin pathways: pharmacodynamics and adverse effects. *Pharmacogen Genom* 21(7):440–446. <https://doi.org/10.1097/FPC.0b013e32833ffb56>
- Verhulst P-F (1838) Notice sur la loi que la population poursuit dans son accroissement. *Corr Math Phys* 10:113–121
- Wang D, Hensman J, Kutkaite G, Toh TS, Galhoz A, Dry JR, Saez-Rodriguez J, Garnett MJ, Menden MP, Dondelinger F (2021) A statistical framework for assessing pharmacological responses and biomarkers using uncertainty estimates. *eLife* 9:60352. <https://doi.org/10.7554/eLife.60352>
- Wu Z, Phan T, Baez J, Kuang Y, Kostelich EJ (2019) Predictability and identifiability assessment of models for prostate cancer under androgen suppression therapy. *Math Biosci Eng* 16(5):3512–3536. <https://doi.org/10.3934/mbe.2019176>
- Zhang L, Sinha V, Forgue ST, Callies S, Ni L, Peck R, Allerheiligen SRB (2006) Model-based drug development: the road to quantitative pharmacology. *J Pharmacokin Pharmacodyn* 33(3):369–393. <https://doi.org/10.1007/s10928-006-9010-8>

Publisher's Note Springer Nature remains neutral with regard to jurisdictional claims in published maps and institutional affiliations.